

Exact solution of the two-axis countertwisting Hamiltonian for the half-integer J case

Feng Pan^{1,3}, Yao-Zhong Zhang^{2,4}, and Jerry P. Draayer³

¹*Department of Physics, Liaoning Normal University, Dalian 116029, P. R. China*

²*School of Mathematics and Physics, The University of Queensland, Brisbane, Qld 4072, Australia*

³*Department of Physics and Astronomy, Louisiana State University, Baton Rouge, Louisiana 70803-4001, USA*

⁴*CAS Key Laboratory of Theoretical Physics, Institute of Theoretical Physics
Chinese Academy of Sciences, Beijing 100190, P. R. China*

(Dated: August 1, 2018)

Bethe ansatz solutions of the two-axis countertwisting Hamiltonian for any (integer and half-integer) J are derived based on the Jordan-Schwinger (differential) boson realization of the $SU(2)$ algebra after desired Euler rotations, where J is the total angular momentum quantum number of the system. It is shown that solutions to the Bethe ansatz equations can be obtained as zeros of the extended Heine-Stieltjes polynomials. Two sets of solutions, with solution number being $J + 1$ and J respectively when J is an integer and $J + 1/2$ each when J is a half-integer, are obtained. Properties of the zeros of the related extended Heine-Stieltjes polynomials for half-integer J cases are discussed. It is clearly shown that double degenerate level energies for half-integer J are symmetric with respect to the $E = 0$ axis. It is also shown that the excitation energies of the ‘yrast’ and other ‘yrare’ bands can all be asymptotically given by quadratic functions of J , especially when J is large.

PACS numbers: 42.50.Dv, 42.50.Lc, 32.60.+i

I. INTRODUCTION

Spin-squeezed states of both Bose and Fermi many-body systems [1–12] have been attracting great attention. Two different models for dynamical generation of spin-squeezed states were proposed in [1]: the one-axis twisting and the two-axis countertwisting Hamiltonians. As shown in [1], the latter model gives rise to maximal squeezing with a squeezing angle independent of system size or evolution time. Although its experimental implementation has not yet been achieved, it is interesting to obtain exact solutions of the two-axis countertwisting Hamiltonian for arbitrary total angular momentum J .

The Bethe ansatz method provides a powerful tool for generating analytic solutions of a solvable model. This method was proposed to solve the Hamiltonian of many-spin chain with nearest neighbor interactions [13], which was further developed by many researchers (see e.g. [14, 15] and references therein). Many-spin systems with a special type of long-range interactions were also solved exactly by Gaudin in [16]. The Gaudin solutions turned out to be equivalent to Richardson’s solutions for a nuclear mean-field of the one-body type plus equal strength pairing interactions among all nucleon pairs [17, 18], in which the pairing algebra is the quasi-spin $SU(2)$. In the Gaudin-Richardson type models [16–18], the one-body terms, which generally can be expressed as a linear combination of the $SU(2)$ generators, appear in the Hamiltonians. These one-body terms are essential in the derivation of their algebraic Bethe ansatz solutions. However, there is no such one-body term in the two-axis countertwisting Hamiltonian.

In fact, the two-axis countertwisting Hamiltonian is equivalent to a special case of the Lipkin-Meshkov-Glick (LMG) model [19, 20] after an Euler rotation. As shown previously, similar to other many-spin systems [13, 16–18], the LMG model can be solved analytically by using the algebraic Bethe ansatz [21, 22]. The same problem can also be solved by using the Dyson boson realization of the $SU(2)$ algebra [19, 20, 23], of which the solutions may be obtained from the Riccati differential equations [19, 20]. Discrete phase analysis of the model with applications to spin squeezing and entanglement was studied in [24]. It was also shown [25] that asymmetric rotor Hamiltonian can be solved analytically by using the algebraic Bethe ansatz. However, as noted in [26], the procedures used in [21, 25] can not be applied to the two-axis countertwisting Hamiltonian directly mainly due to, as mentioned above, the lack of one-body terms in the two-axis countertwisting Hamiltonian.

Recently the two-axis countertwisting spin squeezing Hamiltonian was solved exactly for the integer J case [26], where the algebraic Bethe ansatz is established based on the $SU(1,1)$ algebraic structure. This is achieved by a combination of the Jordan-Schwinger (differential) boson realization of the $SU(2)$ algebra and the Fock-Bargmann correspondence. The procedure not only reveals that the Hamiltonian in this case is exactly solvable, but also shows that the eigenvalue problem can be simplified. Specifically, for integer J , the $2J + 1$ dimensional eigenvalue problem is reduced to finding zeros of four independent one-variable polynomials of $\text{Int}[J/2]$ or $\text{Int}[J/2 + 1]$ order, where $\text{Int}[p]$ is the integer part of p , due to the underlying hidden $SU(1,1)$ symmetry with four different boson seniority number configurations.

However, as already noted in [26], the boson mapping procedure there only works for the integer J case. This can also be seen from the material presented between Eq. (1) and Eq. (7) below, which gives a brief review of the boson mapping in [26]. In this work, we overcome the shortcomings in the procedure of [26] by performing a different boson mapping combined with desired Euler rotations and show that the two-axis countertwisting Hamiltonian can also be exactly solved for half-integers J . One of the keys is introducing two additional parameters in the boson realization so that the Bethe ansatz can be applied without any constraint on the J values. Thus our procedure here works for both integer and half-integer J cases of the two-axis countertwisting model. It will be shown that the $SU(1,1)$ algebraic structure after the suitable transformations is also crucial in the process. Since solutions for the integer J case have already been shown in [26], we will mainly focus on solutions for half-integer J cases in this work. Properties of zeros of the related extended Heine-Stieltjes polynomials for half-integer J will be discussed. It will be shown that double degenerate level energies for half-integer J cases are symmetric with respect to the $E = 0$ axis. It is also shown that the excitation energies of the ‘yrast’ and other ‘yrare’ bands of the system defined can all be asymptotically given by quadratic functions of J , especially when J is large.

II. THE TWO-AXIS COUNTERTWISTING HAMILTONIAN

The two-axis countertwisting Hamiltonian may be written as [1]

$$H_{\text{TA}} = \chi(J_x J_y + J_y J_x), \quad (1)$$

where J_x and J_y , together with J_z , are the total angular momentum operators of the system and χ is a constant. The Hamiltonian (1) is invariant under both parity and time reversal transformations, namely, it is PT -symmetric. Due to time-reversal symmetry, level energies of the system are all doubly degenerate when the quantum number J of the total angular momentum is a half-integer or when $J \rightarrow \infty$ for integer J case [26]. As clearly shown in (1), the Hamiltonian only contains quadratic terms of J_x and J_y , for which the Bethe ansatz method [16–18] for solving the Gaudin-Richardson model can not be applied directly.

In our recent paper [26], it has been shown that the Hamiltonian (1) can be expressed in terms of the Bargmann variables as

$$H_{\text{TA}} = \frac{\chi}{i} \left((1 + 2\delta_{\hat{\nu}_B 1}) z_1 \frac{\partial}{\partial z_2} - (1 + 2\delta_{\hat{\nu}_A 1}) z_2 \frac{\partial}{\partial z_1} + 2z_1 z_2 \left(\frac{\partial^2}{\partial z_2^2} - \frac{\partial^2}{\partial z_1^2} \right) \right), \quad (2)$$

where $\hat{\nu}_A$ and $\hat{\nu}_B$ are seniority number operator of A - and B -bosons, respectively, $i = \sqrt{-1}$, and z_j ($j = 1, 2$) are Bargmann variables with the mapping:

$$A^{\dagger 2} \mapsto z_1, \quad B^{\dagger 2} \mapsto z_2 \quad (3)$$

after the Jordan-Schwinger realization of the $SU(2)$ algebra with

$$J_+ = J_x + iJ_y = A^{\dagger} B, \quad J_- = J_x - iJ_y = B^{\dagger} A, \quad J_0 = J_z = \frac{1}{2}(A^{\dagger} A - B^{\dagger} B), \quad (4)$$

where A^{\dagger} (A) and B^{\dagger} (B) are the boson creation (annihilation) operators. In (2), the seniority number ν_A and ν_B can be taken as 0 or 1, among which the configurations with $\nu_A = \nu_B$ and those with $\nu_A \neq \nu_B$ are related to integer J and half-integer J cases, respectively. Most notably, the one-body term appears in (2), for which the Bethe ansatz method of Gaudin-Richardson becomes applicable. Nevertheless, not only the Hamiltonian (2) is non-Hermitian, but also it can not be expressed in terms of orthonormalized boson modes when $\nu_A \neq \nu_B$ as shown in [26]. Therefore, the boson-realization (2) seems not suitable for half-integer J case of the Hamiltonian (1). When $\nu_A = \nu_B$, which are related to integer J case, however, with further mapping the Bargmann variables $\{z_1, z_2\}$ to new boson operators: $z_1 \mapsto c^{\dagger}$, $\partial/\partial z_1 \mapsto c$, $z_2 \mapsto d^{\dagger}$, $\partial/\partial z_2 \mapsto d$, (2) may be written as

$$H_{\text{TA}} = \chi \left((1 + 2\delta_{\hat{\nu} 1}) (a_1^{\dagger} a_1 - a_2^{\dagger} a_2) + (a_1^{\dagger 2} - a_2^{\dagger 2}) (a_1^2 + a_2^2) \right), \quad (5)$$

where

$$a_1^{\dagger} = \sqrt{\frac{1}{2}}(c^{\dagger} + id^{\dagger}), \quad a_2^{\dagger} = \sqrt{\frac{1}{2}}(c^{\dagger} - id^{\dagger}) \quad (6)$$

are two canonical orthonormal boson modes. Though (5) is still non-Hermitian, its eigenvalues are all real, mainly because of its equivalence to the original Hamiltonian (1) for this case. Since $\nu_A = \nu_B \equiv \nu = 0$ or 1, the total angular momentum of the system should be integer in this case with $J = 0, 1, 2, \dots$. In other words, the Hamiltonian (5) is equivalent to the original one (1) only for integer J values. As shown in [26], Hamiltonian (5), when expressed in terms of $SU(1,1)$ generators, contains a one-body term and can thus be solved exactly by using the Bethe ansatz method for the four different configurations separately.

Since the above boson mapping procedure can not be applied to the half-integer J case, we need to find an alternative way to solve the problem. Actually, after rotation around z axis by $-\pi/4$ with

$$J_x = \sqrt{\frac{1}{2}}J_{x'} - \sqrt{\frac{1}{2}}J_{y'}, \quad J_y = \sqrt{\frac{1}{2}}J_{y'} + \sqrt{\frac{1}{2}}J_{x'}, \quad J_z = J_{z'}, \quad (7)$$

(1) can be expressed as

$$H'_{\text{TA}} = \chi(J_{x'}^2 - J_{y'}^2), \quad (8)$$

which is equivalent to a special LMG model whose large J limit was analyzed in [19, 20] by using the Dyson boson (differential) realization and the corresponding Riccati differential equations.

Then, after further rotation of the system around x' axis by $-\pi/2$ with

$$J_{x''} = J_{x'}, \quad J_{y''} = -J_{z'}, \quad J_{z''} = J_{y'}, \quad (9)$$

(8) becomes

$$H = H''_{\text{TA}} = \chi(J_{x''}^2 - J_{z''}^2) = \chi\left(\frac{1}{4}(J_+^2 + J_-^2) + \frac{1}{2}C_2 - \frac{3}{2}J_0^2\right), \quad (10)$$

where $J_{\pm} = J_{x''} \pm iJ_{y''}$, $J_0 = J_{z''}$, and $C_2 = \frac{1}{2}(J_+J_- + J_-J_+) + J_0^2$ is the Casimir operator of the $SU(2)$ generated by $J_{\pm,0}$. Therefore, up to the Euler rotations, the Hamiltonian (1) is equivalent to (10).

Similar to [26], by using the Jordan-Schwinger realization of $SU(2)$

$$J_+ = a^\dagger b, \quad J_- = b^\dagger a, \quad J_0 = \frac{1}{2}(a^\dagger a - b^\dagger b), \quad (11)$$

where a , b and a^\dagger , b^\dagger are boson annihilation and creation operators, (10) can be expressed as

$$H = \frac{\chi}{4} \left(a^{\dagger 2} b^2 + b^{\dagger 2} a^2 + 2C_2 - \frac{3}{2}(n_a - n_b)^2 \right). \quad (12)$$

Here $n_a = a^\dagger a$ and $n_b = b^\dagger b$ are number operators of a -bosons and b -bosons, respectively.

Introducing two nonzero parameters c_1 and c_2 , we have the following identities:

$$\begin{aligned} a^{\dagger 2} b^2 + b^{\dagger 2} a^2 &= \frac{1}{c_1 c_2} ((c_1 a^{\dagger 2} + c_2 b^{\dagger 2})(c_1 a^2 + c_2 b^2) - c_1^2 n_a(n_a - 1) - c_2^2 n_b(n_b - 1)), \\ n_a n_b &= \frac{1}{c_1^2 + c_2^2} ((c_1^2 n_a + c_2^2 n_b)(n_a + n_b) - c_1^2 n_a^2 - c_2^2 n_b^2). \end{aligned} \quad (13)$$

Then (12) can be expressed as

$$\begin{aligned} H &= \frac{\chi}{4} \left\{ \frac{1}{c_1 c_2} (c_1 a^{\dagger 2} + c_2 b^{\dagger 2})(c_1 a^2 + c_2 b^2) + \frac{1}{c_1 c_2} (c_1^2 n_a + c_2^2 n_b) \right. \\ &\quad - \left(\frac{c_1}{c_2} + \frac{3}{2} + \frac{(3+2\lambda)c_1^2}{c_1^2 + c_2^2} - \lambda \right) n_a^2 - \left(\frac{c_2}{c_1} + \frac{3}{2} + \frac{(3+2\lambda)c_2^2}{c_1^2 + c_2^2} - \lambda \right) n_b^2 \\ &\quad \left. + \frac{3+2\lambda}{c_1^2 + c_2^2} (c_1^2 n_a + c_2^2 n_b)(n_a + n_b) - \lambda(n_a + n_b)^2 + 2C_2 \right\}, \end{aligned} \quad (14)$$

which is independent of c_1 , c_2 , and λ , and can be simplified to the desired form

$$\begin{aligned} H &= \frac{\chi}{4} \left\{ \frac{1}{c_1 c_2} (c_1 a^{\dagger 2} + c_2 b^{\dagger 2})(c_1 a^2 + c_2 b^2) + \frac{1}{c_1 c_2} (c_1^2 n_a + c_2^2 n_b) \right. \\ &\quad \left. + \frac{3+2\lambda}{c_1^2 + c_2^2} (c_1^2 n_a + c_2^2 n_b)(n_a + n_b) - \lambda(n_a + n_b)^2 + 2C_2 \right\} \end{aligned} \quad (15)$$

if

$$\frac{c_1}{c_2} + \frac{3}{2} + \frac{(3+2\lambda)c_1^2}{c_1^2 + c_2^2} - \lambda = 0, \quad \frac{c_2}{c_1} + \frac{3}{2} + \frac{(3+2\lambda)c_2^2}{c_1^2 + c_2^2} - \lambda = 0 \quad (16)$$

are satisfied. There are two sets of solutions to (16), $\lambda = \frac{3}{2}$, $c_1/c_2 = -3 \pm 2\sqrt{2}$, of which any set may be used for our purpose. In the following, we choose

$$\lambda = 3/2, \quad c_2 = 1, \quad c_1 = -3 + 2\sqrt{2}. \quad (17)$$

Then, (15) can be written as

$$H = \frac{\chi}{4} \left(\frac{4}{c_1 c_2} S^+ S^- + \left(\frac{1}{c_1 c_2} + \frac{12J}{c_1^2 + c_2^2} \right) \left(2S^0 - \frac{1}{2}(c_1^2 + c_2^2) \right) - 2J(2J-1) \right), \quad (18)$$

where use has been made of $n_a + n_b = 2J$ and $C_2 = J(J+1)$ for a given quantum number of the total angular momentum J ; moreover

$$S^\pm = c_1 S_a^\pm + c_2 S_b^\pm, \quad S^0 = c_1^2 S_a^0 + c_2^2 S_b^0, \quad (19)$$

and

$$\begin{aligned} S_a^+ &= \frac{1}{2} a^{\dagger 2}, & S_a^- &= \frac{1}{2} a^2, & S_a^0 &= \frac{1}{2} (a^\dagger a + \frac{1}{2}), \\ S_b^+ &= \frac{1}{2} b^{\dagger 2}, & S_b^- &= \frac{1}{2} b^2, & S_b^0 &= \frac{1}{2} (b^\dagger b + \frac{1}{2}) \end{aligned} \quad (20)$$

are respectively $SU_a(1,1)$ and $SU_b(1,1)$ generators which satisfy the commutation relations

$$[S_\rho^0, S_{\rho'}^\pm] = \delta_{\rho\rho'} S_\rho^\pm, \quad [S_\rho^+, S_{\rho'}^-] = -\delta_{\rho\rho'} 2S_\rho^0. \quad (21)$$

It is obvious that the one-body term S^0 appears in (18) after the transformation (13) with the constraints (16). Such one-body term is essential in the Bethe ansatz approach described in [16–18, 21, 25, 26]. The main difference between the boson realizations (18) and (5) lies in the fact that the former introduces two additional parameters c_1 and c_2 with the constraint (17), with which the the Bethe ansatz approach described in [16–18, 21, 25, 26] can now be applied for both the integer and half-integer J cases.

Similar to what is shown in [26], (18) can now be diagonalized via the Bethe ansatz

$$|k, \nu_a, \nu_b; \zeta\rangle = S^+(w_1^{(\zeta)}) S^+(w_2^{(\zeta)}) \cdots S^+(w_k^{(\zeta)}) |\nu_a, \nu_b\rangle \quad (22)$$

with $J = k + \frac{1}{2}(\nu_a + \nu_b)$, where $|\nu_a, \nu_b\rangle$ is the lowest weight state of the $SU_\rho(1,1)$ for $\rho = a$ and b , satisfying $S_\rho^- |\nu_a, \nu_b\rangle = 0$ and $2S_\rho^0 |\nu_a, \nu_b\rangle = (\nu_\rho + \frac{1}{2}) |\nu_a, \nu_b\rangle$ with $\nu_\rho = 0$ or 1 , and

$$S^+(w) = \frac{c_1}{1 - c_1^2 w} S_a^+ + \frac{c_2}{1 - c_2^2 w} S_b^+. \quad (23)$$

Using the commutation relations (21), it can be proven that

$$[S^0, S^+(w)] = \frac{c_1^3}{1 - c_1^2 w} S_a^+ + \frac{c_2^3}{1 - c_2^2 w} S_b^+ = \frac{1}{w} (S^+(w) - S^+), \quad (24)$$

$$[S^-, S^+(w)] = \Lambda_0(w) = \frac{2c_1^2 S_a^0}{1 - c_1^2 w} + \frac{2c_2^2 S_b^0}{1 - c_2^2 w}, \quad (25)$$

$$S^+(w_1, w_2) = [[S^-, S^+(w_1)], S^+(w_2)] = \frac{2}{w_1 - w_2} (S^+(w_1) - S^+(w_2)). \quad (26)$$

With the help of (24)-(26), we can directly check that

$$\begin{aligned} S^0|k, \nu_a, \nu_b; \zeta\rangle &= \frac{1}{w_1^{(\zeta)}} \left(S^+(w_1^{(\zeta)}) - S^+ \right) S^+(w_2^{(\zeta)}) \cdots S^+(w_k^{(\zeta)}) |\nu_a, \nu_b\rangle \\ &\quad + \cdots + S^+(w_1^{(\zeta)}) \cdots S^+(w_{k-1}^{(\zeta)}) \frac{1}{w_k^{(\zeta)}} \left(S^+(w_k^{(\zeta)}) - S^+ \right) |\nu_a, \nu_b\rangle, \end{aligned} \quad (27)$$

and

$$\begin{aligned} S^+ S^- |k, \nu_a, \nu_b; \zeta\rangle &= S^+ \left(\bar{\Lambda}_0(w_1^{(\zeta)}) S^+(w_2^{(\zeta)}) \cdots S^+(w_k^{(\zeta)}) \right. \\ &\quad + \cdots + S^+(w_1^{(\zeta)}) \cdots S^+(w_{k-1}^{(\zeta)}) \bar{\Lambda}_0(w_k^{(\zeta)}) \Big) |\nu_a, \nu_b\rangle \\ &\quad + S^+ \left(S_+(w_1^{(\zeta)}, w_2^{(\zeta)}) S^+(w_3^{(\zeta)}) \cdots S^+(w_k^{(\zeta)}) \right. \\ &\quad + S^+(w_1^{(\zeta)}, w_3^{(\zeta)}) S^+(w_2^{(\zeta)}) S_+(w_4^{(\zeta)}) \cdots S^+(w_k^{(\zeta)}) \\ &\quad + \cdots + S_+(w_1^{(\zeta)}, w_k^{(\zeta)}) S_+(w_2^{(\zeta)}) \cdots S^+(w_{k-1}^{(\zeta)}) \\ &\quad + \cdots + S_+(w_k^{(\zeta)}, w_1^{(\zeta)}) S_+(w_2^{(\zeta)}) \cdots S^+(w_{k-1}^{(\zeta)}) \\ &\quad + S^+(w_k^{(\zeta)}, w_2^{(\zeta)}) S_+(w_3^{(\zeta)}) \cdots S^+(w_{k-1}^{(\zeta)}) \\ &\quad \left. + \cdots + S^+(w_k^{(\zeta)}, w_{k-1}^{(\zeta)}) S^+(w_2^{(\zeta)}) \cdots S^+(w_{k-2}^{(\zeta)}) \right) |\nu_a, \nu_b\rangle, \end{aligned} \quad (28)$$

where $\bar{\Lambda}_0(w) = \frac{c_1^2(\nu_a + \frac{1}{2})}{1 - c_1^2 w} + \frac{c_2^2(\nu_b + \frac{1}{2})}{1 - c_2^2 w}$.

Now by means of (26)-(28), we can prove that the eigen-equation $H|k, \nu_a, \nu_b; \zeta\rangle = E_{k, \nu_a, \nu_b}^{(\zeta)} |k, \nu_a, \nu_b; \zeta\rangle$ is fulfilled if and only if

$$\frac{(\nu_a + \frac{1}{2})c_1^2}{1 - c_1^2 w_l^{(\zeta)}} - \left(\frac{1}{2} + \frac{6c_1 c_2 J}{c_1^2 + c_2^2} \right) \frac{1}{w_l^{(\zeta)}} + \frac{(\nu_b + \frac{1}{2})c_2^2}{1 - c_2^2 w_l^{(\zeta)}} - \sum_{j \neq l} \frac{2}{w_l^{(\zeta)} - w_j^{(\zeta)}} = 0 \quad \text{for } l = 1, 2, \dots, k. \quad (29)$$

The corresponding eigen-energy is given by

$$E_{k, \nu_a, \nu_b}^{(\zeta)} = \frac{\chi}{4} \left\{ \left(\frac{1}{c_1 c_2} + \frac{12J}{c_1^2 + c_2^2} \right) \left(\sum_{l=1}^k \frac{2}{w_l^{(\zeta)}} + c_1^2 \nu_a + c_2^2 \nu_b \right) - 2J(2J - 1) \right\} \quad (30)$$

with $J = k + \frac{1}{2}(\nu_a + \nu_b)$, where k is the number of boson pairs, while $\nu_a + \nu_b$ are the total number of unpaired bosons. It can be inferred from (30) that the spectrum of the Hamiltonian (18) is generated from the non-linear boson-pair excitations based on the single-boson excitations, while the single-boson excitation energies contribute to the total energy linearly. Moreover, it is obvious that Eq. (29) and the eigenvalues (30) are invariant under the simultaneous interchanges $\nu_a \leftrightarrow \nu_b$ and $c_1 \leftrightarrow c_2$. Actually, the eigenvalues of (14) for $\{\nu_a = 1, \nu_b = 0\}$ should be the same as those for $\{\nu_a = 0, \nu_b = 1\}$ since the Hamiltonian (14) and the constraints (16) are all invariant under the permutation of c_1 and c_2 , which clearly shows that each level energy is doubly degenerate when J is a half-integer. Hence, we only need to solve one of the cases for half-integer J . The results of the other case can be obtained by permuting the a -bosons with the b -bosons. In addition, as shown previously [27–29], though the eigenstates provided in (22) are not normalized, they are always orthogonal with

$$\langle k', \nu'_a, \nu'_b; \zeta' | k, \nu_a, \nu_b; \zeta \rangle = (\mathcal{N}(k, \zeta; \nu_a, \nu_b))^{-2} \delta_{kk'} \delta_{\nu_a \nu'_a} \delta_{\nu_b \nu'_b} \delta_{\zeta \zeta'}, \quad (31)$$

where $\mathcal{N}(k, \zeta; \nu_a, \nu_b)$ is the corresponding normalization constant.

According to the Heine-Stieltjes correspondence [27–29], roots of (29) are zeros of the extended Heine-Stieltjes polynomials $y_k(w)$ of degree k satisfying the following second-order Fuchsian equation:

$$y_k''(w) + \left(\frac{\nu_a + \frac{1}{2}}{w - c_1} + \frac{\nu_b + \frac{1}{2}}{w - c_2} + \frac{\gamma_J}{w} \right) y_k'(w) + \frac{V(w)}{w(1 - c_1^2 w)(1 - c_2^2 w)} y_k(w) = 0, \quad (32)$$

where

$$\gamma_J = 1/2 + \frac{6c_1 c_2 J}{c_1^2 + c_2^2} = \frac{1}{2} - J, \quad (33)$$

and $V(w)$ is a Van Vleck polynomial of degree 1 determined according to (32). Therefore, the Heine-Stieltjes polynomial approach for solving the Gaudin-Richardson type equations as shown in [27–29] is applicable for solving the Bethe ansatz equations (29). It should be noted that a similar approach for solving the Gaudin-Richardson type equations has been proposed in Ref. [31, 32], which however requires the solutions of a set of higher-order differential equations. Further discussions about the similarities and the differences of the Heine-Stieltjes polynomial approach and the method shown in [31, 32] may be found in [29, 30]. Since $\nu_a + \frac{1}{2}$ and $\nu_b + \frac{1}{2}$ are always real and positive, while γ_J is negative except for $J = 1/2$, zeros of the extended Heine-Stieltjes polynomials may be complex. Let the absolute values of the real parts of these complex zeros be arranged as $|\operatorname{Re}[w_1]| < |\operatorname{Re}[w_2]| < \dots < |\operatorname{Re}[w_k]|$, which are in the union of two open intervals: $\{|\operatorname{Re}[w_1]|, |\operatorname{Re}[w_2]|, \dots, |\operatorname{Re}[w_k]| \} \in (0, 1) \cup (1, c_1^{-2})$ (noticing that $c_1^{-2} > c_2^{-2} = 1$).

An electrostatic interpretation of the location of zeros of $y_k(w)$ may be stated as follows. Put two positive fractional charges $\frac{1}{2}\nu_a + \frac{1}{4}$, $\frac{1}{2}\nu_b + \frac{1}{4}$ at c_1^{-2} and 1, and one negative fractional charge $\frac{1}{4} - \frac{J}{2}$ at 0 along a real axis of a two-dimensional complex plane, respectively, and allow k positive unit charges to move freely on the entire two-dimensional complex plane. There are $k+1$ different configurations for the positions of these k positive unit charges, of which the absolute values of the real parts $\{|\operatorname{Re}[w_1^{(\zeta)}]|, \dots, |\operatorname{Re}[w_k^{(\zeta)}]| \}$ with $\zeta = 1, 2, \dots, k+1$, correspond to global minimums of the total electrostatic energy of the system [27], though the imaginary parts of these zeros can not be determined beforehand. The total number of these configurations is exactly the number of ways to put the k absolute values of the real parts of the complex zeros into the two open intervals, which is $k+1$. Thus, there are $k+1$ different polynomials $y_k(w)$ for given $\{\nu_a, \nu_b\}$. Since $0 \leq \nu_a, \nu_b \leq 1$, for a given integer $J = k$, there are $k+1$ solutions for the case with $\{\nu_a = \nu_b = 0\}$, while there are k solutions for the case with $\{\nu_a = \nu_b = 1\}$. When J is a half-integer with $J = k + 1/2$, there are $k+1$ solutions for the case with $\{\nu_a = 1, \nu_b = 0\}$ or $\{\nu_a = 0, \nu_b = 1\}$. Hence, the total number of different solutions equals exactly to $2J+1$ for both integer and half-integer J cases, which proves the completeness of the solutions provided by (29) for the Hamiltonian (10). Fig. 1 provides two possible configurations of the 10 roots for $J = 21/2$ ($k = 10$) case with $\{\nu_a = 0, \nu_b = 1\}$ corresponding to the ground and the first excited states, which clearly shows that the absolute values of the real parts of the roots indeed fall into the union of the two open intervals $(0, 1) \cup (1, c_1^{-2})$. It can be observed that the solutions provided by (29) are complex in general in contrast to the integer J case provided in [26], of which the solutions are always real.

Once the Bethe ansatz equations (29) are solved, the eigenstates (22), up to a normalization constant, can be expressed in terms of the original a - and b -boson operators as

$$|k, \nu_a, \nu_b; \zeta\rangle = \sum_{\rho=0}^k B_{\rho}^{(k)} c_1^{\rho} a^{\dagger 2k-2\rho} b^{\dagger 2\rho} |\nu_a, \nu_b\rangle, \quad (34)$$

where $c_2 = 1$ has been used,

$$B_{\rho}^{(k)} = \sum_{q=0}^k (-)^q S_q^{(k, \zeta)} \sum_{\mu=0}^{\min[\rho, k-q]} \binom{k-q}{\mu} \binom{q}{\rho-\mu} c_1^{-2\mu}, \quad (35)$$

and

$$S_0^{(k, \zeta)} = 1, \quad S_{q \geq 1}^{(k, \zeta)} = \sum_{1 \leq \mu_1 \neq \dots \neq \mu_q \leq k} w_{\mu_1}^{(\zeta)} \dots w_{\mu_q}^{(\zeta)} \quad (36)$$

are symmetric functions in $\{w_1^{(\zeta)}, \dots, w_k^{(\zeta)}\}$, which are related to the expansion coefficients of $y_k(w)$ when it is expanded in terms of powers of w [27–29]. Thus, when $J = k$, we have

$$|J = k, \zeta\rangle = \begin{cases} \sum_{\rho=0}^k \frac{B_{\rho}^{(k)} c_1^{\rho}}{((2k-2\rho)!(2\rho)!)^{-\frac{1}{2}}} |J = k, M = k - 2\rho\rangle & \text{for } \nu_a = \nu_b = 0, \\ \sum_{\rho=0}^{k-1} \frac{B_{\rho}^{(k-1)} c_1^{\rho}}{((2k-2\rho-1)!(2\rho+1)!)^{-\frac{1}{2}}} |J = k, M = k - 2\rho - 1\rangle & \text{for } \nu_a = \nu_b = 1. \end{cases} \quad (37)$$

When $J = k + 1/2$, we have

$$|J = k + 1/2, \zeta\rangle = \begin{cases} \sum_{\rho=0}^k \frac{B_{\rho}^{(k)} c_1^{\rho}}{((2k-2\rho+1)!(2\rho)!)^{-\frac{1}{2}}} |J = k + \frac{1}{2}, M = k - 2\rho + \frac{1}{2}\rangle & \text{for } \nu_a = 1, \nu_b = 0, \\ \sum_{\rho=0}^k \frac{B_{\rho}^{(k)} c_1^{\rho}}{((2k-2\rho)!(2\rho+1)!)^{-\frac{1}{2}}} |J = k + \frac{1}{2}, M = k - 2\rho - \frac{1}{2}\rangle & \text{for } \nu_a = 0, \nu_b = 1. \end{cases} \quad (38)$$

It is clear that there are two set of solutions for the half-integer case, instead of four sets for the integer J case as shown in [26].

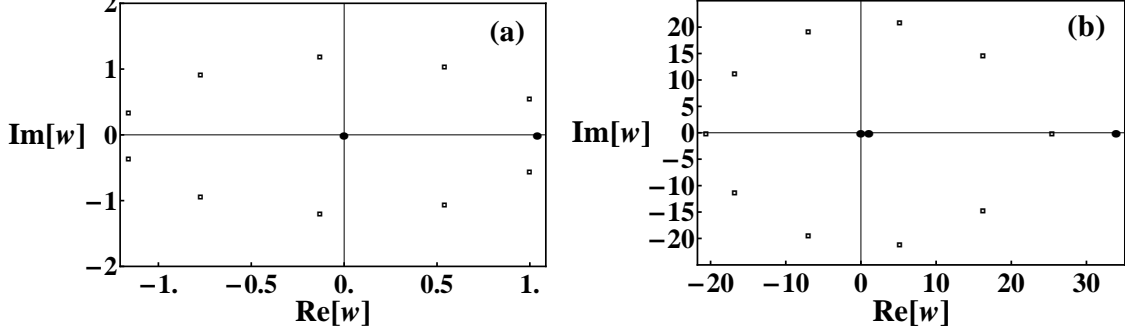


FIG. 1: The two possible configurations of 10 zeros of the extended Heine-Stieltjes polynomial $y_{10}^{(\zeta)}(w)$ for $J = 21/2$ ($k = 10$) case with $\{\nu_a = 0, \nu_b = 1\}$ corresponding to the ground and the first excited states of the system, where the solid dot at 0 on the real axis represents the negative charge $\gamma_J = 1/2 - J$ when $J \geq 1/2$, those at 1 and c_1^{-2} on the real axis represent the charges $\nu_b + \frac{1}{2} = \frac{3}{2}$ and $\nu_a + \frac{1}{2} = \frac{1}{2}$, respectively, the open squares represent the possible positions of the 10 positive unit charges or zeros of the polynomial, (a) the positions of the 10 zeros of $y_{10}^{(\zeta=1)}(w)$ for the ground state with eigen-energy $E_{10,1,0}^{(\zeta=1)}/\chi = -105.948$, in which the positive charge $\frac{1}{2}$ at $c_1^{-2} = 33.9706$ is not shown, and (b) the positions of the 10 zeros of $y_{10}^{(\zeta=2)}(w)$ for the first excited state with eigen-energy $E_{10,1,0}^{(\zeta=2)}/\chi = -77.8789$.

To solve (29) more easily, as shown in [27–30] for the extended Heine-Stieltjes polynomials, we may simply write

$$y_k^{(\zeta)}(w) = \sum_{j=0}^k b_j^{(\zeta)} w^j, \quad (39)$$

where $\{b_j^{(\zeta)}\}$ ($j = 0, 1, \dots, k$) are the ζ -th set of the expansion coefficients to be determined. Substitution of (39) into (32) yields the equation which determine the corresponding Van Vleck polynomial as

$$V^{(\zeta)}(w) = c_1^2 k(J - k - \frac{1}{2} - \nu_a - \nu_b)w + g_0^{(\zeta)}. \quad (40)$$

The expansion coefficients $b_j^{(\zeta)}$ and $g_0^{(\zeta)}$ satisfy the following three-term recurrence relation:

$$(J - j - 1/2)(j + 1)b_{j+1}^{(\zeta)} + c_1^2(k + 1 - j)(\nu_a + \nu_b + k + j - J - 1/2)b_{j-1}^{(\zeta)} + j((c_1^2 + 1)(j - 1) + \alpha)b_j^{(\zeta)} = g_0^{(\zeta)}b_j^{(\zeta)} \quad (41)$$

where $b_j^{(\zeta)} = 0$ for $j \leq -1$ or $j \geq k + 1$ and $\alpha = c_1^2(\nu_a - J + 1) + \nu_b - J + 1$. The recurrence (41) is equivalent to the eigenvalue problem

$$\mathbf{F}\mathbf{b}^{(\zeta)} = g_0^{(\zeta)}\mathbf{b}^{(\zeta)}, \quad (42)$$

where the transpose of $\mathbf{b}^{(\zeta)}$ is related to the expansion coefficients $\{b_j^{(\zeta)}\}$ with $(\mathbf{b}^{(\zeta)})^T = (b_0^{(\zeta)}, b_1^{(\zeta)}, \dots, b_{k-1}^{(\zeta)}, b_k^{(\zeta)})$ and \mathbf{F} is the $(k + 1) \times (k + 1)$ tridiagonal matrix with entries determined by (41).

In addition, (39) can also be written in terms of the zeros $\{w_j^{(\zeta)}\}$ ($j = 1, \dots, k$) of $y_k^{(\zeta)}(w)$ as

$$y_k^{(\zeta)}(w) = \prod_{j=1}^k (w - w_j^{(\zeta)}) = \sum_{q=0}^k (-1)^q S_q^{(k, \zeta)} w^{k-q}, \quad (43)$$

where $S_q^{(k,\zeta)}$ is the symmetric function defined in (36). Comparing (43) with (39), we get

$$S_q^{(k,\zeta)} = (-1)^q b_{k-q}^{(\zeta)} \quad (44)$$

if the overall factor of $\{b_j^{(\zeta)}\}$ is chosen to be $b_k^{(\zeta)} = 1 \forall \zeta$, which can be used for the eigenstates (37) and (38) to avoid unnecessary computation of $S_q^{(k,\zeta)}$ from $\{w_1^{(\zeta)}, \dots, w_k^{(\zeta)}\}$.

III. SOME NUMERICAL EXAMPLES OF THE SOLUTION

To demonstrate the method and solutions outlined above, in this section, we provide some examples of the solutions of (1) for half-integer cases. Due to time reversal symmetry, two sets of the solutions with $\{\nu_a = 0, \nu_b = 1\}$ and $\{\nu_a = 1, \nu_b = 0\}$ are degenerate for any half-integer J . Actually, eigenstates of the second set of solutions with $\{\nu_a = 1, \nu_b = 0\}$ can be obtained from those with $\{\nu_a = 0, \nu_b = 1\}$ by permuting a -bosons with b -bosons. When $J = 1/2$, the solutions are trivial with $k = 0$. The corresponding eigen-energies are $E_{0,1,0}^{(\zeta)} = E_{0,0,1}^{(\zeta)} = 0$. When $J \geq 3/2$, all solutions are non-trivial. In the following, only some non-trivial $k \neq 0$ solutions for half-inter J cases will be presented.

TABLE I: The Heine-Stieltjes Polynomials $y_k^{(\zeta)}(w)$, $g_0^{(\zeta)}$ of the corresponding Van Vleck Polynomial $V^{(\zeta)}(w)$, and the corresponding eigenenergy $E_{k,\nu_a,\nu_b}^{(\zeta)}/\chi$ of the Hamiltonian (1) for $J \leq 5$, where the order of ζ is arranged according to the value of the eigen-energy of (1) for a given set of $\{k, \nu_a, \nu_b\}$.

J	$\{k, \zeta; \nu_a, \nu_b\}$	$y_k^{(\zeta)}(w)$	$g_0^{(\zeta)}$	$E_{k,\nu_a,\nu_b}^{(\zeta)}/\chi$
3/2	{1, 1; 1, 0}	$18.3378 + w$	0.0545323	-1.73205
	{1, 2; 1, 0}	$-1.85249 + w$	-0.539814	1.73205
	{1, 1; 0, 1}	$1.85249 + w$	0.539814	-1.73205
	{1, 2; 0, 1}	$-18.3378 + w$	-0.0545323	1.73205
5/2	{2, 1; 1, 0}	$448.949 + 17.8348w + w^2$	17.8348	-5.2915
	{2, 2; 1, 0}	$-5.82843 + 2.41421w + w^2$	2.41421	0
	{2, 3; 1, 0}	$14.9816 - 13.0064w + w^2$	-13.0064	5.2915
	{2, 1; 0, 1}	$2.57044 + 1.3495w + w^2$	1.3495	-5.2915
	{2, 2; 0, 1}	$-197.995 - 14.0711w + w^2$	-14.0711	0
	{2, 3; 0, 1}	$77.0275 - 29.4916w + w^2$	-29.4916	5.2915
7/2	{3, 1; 1, 0}	$12572.6 + 445.604w + 17.6893w^2 + w^3$	445.604	-10.8624
	{3, 2; 1, 0}	$-13.2801 + 5.62989w + 2.084w^2 + w^3$	5.62989	-2.83003
	{3, 3; 1, 0}	$113.704 - 85.0097w - 8.91243w^2 + w^3$	-85.0097	2.83003
	{3, 4; 1, 0}	$-80.9492 + 97.7069w - 24.5177w^2 + w^3$	97.7069	10.8624
	{3, 1; 0, 1}	$3.11805 + 1.62364w + 1.204w^2 + w^3$	1.62364	-10.8624
	{3, 2; 0, 1}	$-2951.93 - 181.093w - 14.4013w^2 + w^3$	-181.093	-2.83003
	{3, 3; 0, 1}	$344.772 - 90.4534w - 25.3977w^2 + w^3$	-90.4534	2.83003
	{3, 4; 0, 1}	$-484.279 + 349.521w - 41.003w^2 + w^3$	349.521	10.8624
9/2	{4, 1; 1, 0}	$372346 + 12541.9w + 444.373w^2 + 17.6295w^3 + w^4$	12541.9	-18.4421
	{4, 2; 1, 0}	$-22.883 + 9.993w + 3.49161w^2 + 1.65038w^3 + w^4$	9.993	-7.47579
	{4, 3; 1, 0}	$1154 - 873.992w - 101.912w^2 - 9.24264w^3 + w^4$	-873.992	0
	{4, 4; 1, 0}	$-434.327 + 468.213w - 49.1045w^2 - 20.1357w^3 + w^4$	468.213	7.47579
	{4, 5; 1, 0}	$479.231 - 742.042w + 314.622w^2 - 36.1148w^3 + w^4$	-742.042	18.4421
	{4, 1; 0, 1}	$3.57655 + 1.8561w + 1.37723w^2 + 1.14425w^3 + w^4$	1.8561	-18.4421
	{4, 2; 0, 1}	$-58196.6 - 2827.34w - 176.083w^2 - 14.8349w^3 + w^4$	-2827.34	-7.47579
	{4, 3; 0, 1}	$1154 - 313.978w - 101.912w^2 - 25.7279w^3 + w^4$	-313.978	0
	{4, 4; 0, 1}	$-3066.16 + 1817.43w + 130.47w^2 - 36.6209w^3 + w^4$	1817.43	7.47579
	{4, 5; 0, 1}	$2778.86 - 2954.26w + 757.618w^2 - 52.6001w^3 + w^4$	-2954.26	18.4421

TABLE II: The same as Table I, but for $J = 21/2$.

$\{k, \zeta; \nu_a, \nu_b\}$	$y_k^{(\zeta)}(w)$	$g_0^{(\zeta)}$	$E_{k, \nu_a, \nu_b}^{(\zeta)} / \chi$
$\{10, 1; 1, 0\}$	$3.66943 \times 10^{14} + 1.13715 \times 10^{13}w + 3.54484 \times 10^{11}w^2 + 1.11326 \times 10^{10}w^3 + 3.53008 \times 10^8w^4 + 1.13402 \times 10^7w^5 + 371120w^6 + w^{10}$	1.13715×10^{13}	-105.948
$\{10, 2; 1, 0\}$	$-101.618 + 45.7896w + 15.0023w^2 + 7.07498w^3 + 4.31317w^4 + 2.98896w^5 + 2.22996w^6 + 1.74641w^7 + 1.4158w^8 + 1.17792w^9 + w^{10}$	45.7896	-77.8789
$\{10, 3; 1, 0\}$	$7.80873 \times 10^{10} - 6.86055 \times 10^{10}w - 4.95308 \times 10^9w^2 - 2.71706 \times 10^8w^3 - 1.36749 \times 10^7w^4 - 676937w^5 - 34672.2w^6 - 1969.52w^7 - 141.08w^8 + w^{10}$	-6.86055×10^{10}	-52.9351
$\{10, 4; 1, 0\}$	$-106096 + 132604w - 18511.1w^2 - 6740.2w^3 - 2078.69w^4 - 795.203w^5 - 354.007w^6 - 166.08w^7 - 74.4573w^8 - 25.9728w^9 + w^{10}$	132604	-31.2956
$\{10, 5; 1, 0\}$	$2.55952 \times 10^8 - 3.98371 \times 10^8w + 1.24488 \times 10^8w^2 + 1.85329 \times 10^7w^3 + 1.82955 \times 10^6w^4 + 166734w^5 + 16160.7w^6 + 1698.38w^7 + 113.787w^8 - 36.3873w^9 + w^{10}$	-3.98371×10^8	-13.4271
$\{10, 6; 1, 0\}$	$-7.7618 \times 10^6 + 1.38688 \times 10^7w - 6.12768 \times 10^6w^2 - 197323w^3 + 117925w^4 + 39932.7w^5 + 10231.3w^6 + 2303.31w^7 + 334.544w^8 - 44.2132w^9 + w^{10}$	1.38688×10^7	0
$\{10, 7; 1, 0\}$	$2.16991 \times 10^7 - 4.37708 \times 10^7w + 2.49872 \times 10^7w^2 - 1.87605 \times 10^6w^3 - 824936w^4 - 126530w^5 - 9418.12w^6 + 1486.04w^7 + 623.35w^8 - 52.0391w^9 + w^{10}$	-4.37708×10^7	13.4271
$\{10, 8; 1, 0\}$	$-1.85276 \times 10^7 + 4.30535 \times 10^7w - 3.19566 \times 10^7w^2 + 6.76683 \times 10^6w^3 + 766832w^4 - 98749.6w^5 - 38784.5w^6 - 2953.46w^7 + 1113.23w^8 - 62.4536w^9 + w^{10}$	4.30535×10^7	31.2956
$\{10, 9; 1, 0\}$	$1.87476 \times 10^7 - 5.05252 \times 10^7w + 4.7973 \times 10^7w^2 - 1.78911 \times 10^7w^3 + 1.26629 \times 10^6w^4 + 478782w^5 - 17931.1w^6 - 15528.5w^7 + 1867.83w^8 - 75.066w^9 + w^{10}$	-5.05252×10^7	52.9351
$\{10, 10; 1, 0\}$	$-1.87384 \times 10^7 + 5.85199 \times 10^7w - 6.95261 \times 10^7w^2 + 3.86517 \times 10^7w^3 - 9.50417 \times 10^6w^4 + 389737w^5 + 239926w^6 - 43240w^7 + 2956.95w^8 - 89.6043w^9 + w^{10}$	5.85199×10^7	77.8789
$\{10, 11; 1, 0\}$	$1.87386 \times 10^7 - 6.7545 \times 10^7w + 9.83678 \times 10^7w^2 - 7.47613 \times 10^7w^3 + 3.21533 \times 10^7 \times w^4 - 8.01874 \times 10^6w^5 + 1.16068 \times 10^6w^6 - 96440.7w^7 + 4463.39w^8 - 105.964w^9 + w^{10}$	-6.7545×10^7	105.948
$\{10, 1; 0, 1\}$	$5.57736 + 2.87943w + 2.13913w^2 + 1.77814w^3 + 1.55429w^4 + 1.39809w^5 + 1.28114w^6 + 1.18935w^7 + 1.11482w^8 + 1.05274w^9 + w^{10}$	2.87943	-105.948
$\{10, 2; 0, 1\}$	$-2.01399 \times 10^{13} - 6.98348 \times 10^{11}w - 2.47089 \times 10^{10}w^2 - 8.97212 \times 10^8w^3 - 3.37243 \times 10^7w^4 - 1.33065 \times 10^6w^5 - 56524.7w^6 + w^{10}$	-6.98348×10^{11}	-77.8789
$\{10, 3; 0, 1\}$	$26208.8 - 10307.7w - 3204.1w^2 - 1316.74w^3 - 682.365w^4 - 392.176w^5 - 233.215w^6 - 136.404w^7 - 73.1981w^8 - 29.8456w^9 + w^{10}$	-10307.7	-52.9351
$\{10, 4; 0, 1\}$	$-1.92898 \times 10^{10} + 1.47483 \times 10^{10}w + 1.2446 \times 10^9w^2 + 8.17213 \times 10^7w^3 + 5.12777 \times 10^6w^4 + 339072w^5 + 26091.6w^6 + 2490.47w^7 + 201.344w^8 - 42.4581w^9 + w^{10}$	1.47483×10^{10}	-31.2956
$\{10, 5; 0, 1\}$	$7.99592 \times 10^6 - 8.56477 \times 10^6w + 788414.w^2 + 346414w^3 + 97032.7w^4 + 29469.9w^5 + 9519.11w^6 + 2838.52w^7 + 561.275w^8 - 52.8726w^9 + w^{10}$	-8.56477×10^6	-13.4271
$\{10, 6; 0, 1\}$	$-2.63673 \times 10^8 + 3.43174 \times 10^8w - 7.64386 \times 10^7w^2 - 1.5492 \times 10^7w^3 - 2.02576 \times 10^6w^4 - 232745w^5 - 20232.7w^6 + 996.608w^7 + 911.043w^8 - 60.6985w^9 + w^{10}$	3.43174×10^8	0
$\{10, 7; 0, 1\}$	$9.43159 \times 10^7 - 1.44481 \times 10^8w + 5.09462 \times 10^7w^2 + 3.57526 \times 10^6w^3 - 667019w^4 - 263794w^5 - 50627.8w^6 - 3389.31w^7 + 1328.86w^8 - 68.5244w^9 + w^{10}$	-1.44481×10^8	13.4271
$\{10, 8; 0, 1\}$	$-1.10461 \times 10^8 + 2.03078 \times 10^8w - 1.06558 \times 10^8w^2 + 8.32205 \times 10^6w^3 + 3.21702 \times 10^6w^4 + 241118w^5 - 55117.7w^6 - 14317.7w^7 + 1990.42w^8 - 78.9389w^9 + w^{10}$	2.03078×10^8	31.2956
$\{10, 9; 0, 1\}$	$1.09164 \times 10^8 - 2.41225 \times 10^8w + 1.76691 \times 10^8w^2 - 4.32417 \times 10^7w^3 - 1.46987 \times 10^6w^4 + 1.15533 \times 10^6w^5 + 89949.6w^6 - 37410.9w^7 + 2952.95w^8 - 91.5513w^9 + w^{10}$	-2.41225×10^8	52.9351
$\{10, 10; 0, 1\}$	$-1.09218 \times 10^8 + 2.88085 \times 10^8w - 2.79855 \times 10^8w^2 + 1.20468 \times 10^8w^3 - 1.96771 \times 10^7w^4 - 940918w^5 + 675448w^6 - 80861.7w^7 + 4281.74w^8 - 106.09w^9 + w^{10}$	2.88085×10^8	77.8789
$\{10, 11; 0, 1\}$	$1.09217 \times 10^8 - 3.4068 \times 10^8w + 4.22424 \times 10^8w^2 - 2.68684 \times 10^8w^3 + 9.51901 \times 10^7w^4 - 1.93589 \times 10^7w^5 + 2.28507 \times 10^6w^6 - 156404w^7 + 6057.88w^8 - 122.45w^9 + w^{10}$	-3.4068×10^8	105.948

The Heine-Stieltjes polynomials $y_k^{(\zeta)}(w)$ and the corresponding coefficient $g_0^{(\zeta)}$ in the Van Vleck polynomials (40) up to $J = 9/2$ are shown in Table I, while the $J = 21/2$ case is provided in Table II. For any case, it can be verified that the absolute value of the real part of any zero of $y_k^{(\zeta)}(w)$ indeed lies in one of the intervals $(0, 1)$ and $(1, c_1^{-2})$. When a zero is complex, there must be its complex conjugation as another zero, which is clearly demonstrated in Fig. 1. Thus, eigenvalues (30) are always real. The two-axis countertwisting Hamiltonian can be easily diagonalized by brute force for small value of total angular momentum J , i.e. when the number of particles of the system is small. We can check that the eigen-energies shown in Tables I and II are exactly the same as those given in Table I of [33] obtained from the direct $2J + 1$ dimensional matrix diagonalization for the corresponding half-integer J values.

Furthermore, by using (44), the eigen-energies given in (30) can also be expressed as

$$E_{k,\nu_a,\nu_b}^{(\zeta)} = \frac{\chi}{4} \left\{ \left(\frac{1}{c_1 c_2} + \frac{12J}{c_1^2 + c_2^2} \right) \left(-2b_1^{(\zeta)}/b_0^{(\zeta)} + c_1^2 \nu_a + c_2^2 \nu_b \right) - 2J(2J - 1) \right\} \quad (45)$$

with $J = k + (\nu_a + \nu_b)/2$, of which the corresponding numerical values are also provided in the last column of Tables I and II. It is shown in these Tables that there is an excited state with $E_{k,n_1,n_2,\nu} = 0$ when k is zero or even for $J = k + \frac{1}{2}$, while all excited energies are non-zero when k is odd, which applies to any J .

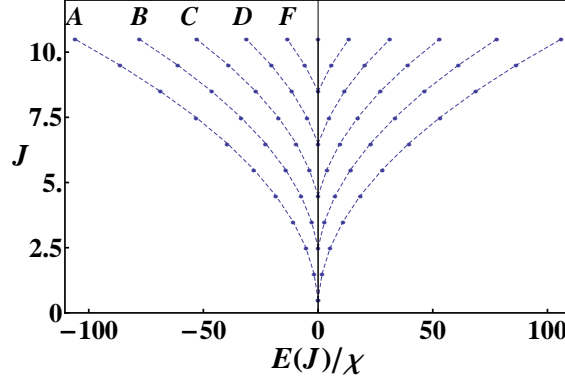


FIG. 2: The level energies $E(J)/\chi$ denoted by solid dots up to $J = 21/2$, where the dots connected by the dashed lines belong to the yrast and yrare bands, of which only the first 5 bands denoted by A to F and their mirror symmetric ones after the reflection with $E(J) \rightarrow -E(J)$ are shown.

As demonstrated in Fig. 2 for level energies of the system up to $J = 21/2$, the level energy distribution for pairs of the double-degenerate levels is symmetric with respect to $E = 0$ axis. There are $\text{Int}[k/2] + 1$ doubly degenerate levels for odd k or $k/2$ doubly degenerate levels for even k with energies $E_r < 0$ and the same number of pairs of doubly degenerate levels with energies $E_r > 0$ for $r = 1, 2, \dots, \text{Int}[k/2] + 1$ when k is odd ($k/2$ when k is even), which is consistent with the conclusion in [26] for integer J cases.

More interestingly, similar to the term used in analyzing energy spectrum of a nucleus [34], we may define the yrast and other yrare bands of the two-axis countertwisting Hamiltonian. The yrast band consists of the double-degenerate minimum (ground state) energies of the system for all possible half-integer J , and the next yrare band consists of the first excitation energies for all possible half-integer J , and so on. For given k with $\nu_a = 0$ and $\nu_b = 1$ for example, according to (45), these yrast and yrare bands are given by

$$E^{(\zeta)}(J)/\chi = - \left(J^2 - (\Omega(\zeta, J) + \frac{1}{2} - \frac{1}{2c_1})J + \frac{1}{2}(\Omega(\zeta, J) - \frac{1}{2c_1}) \right) \quad (46)$$

with $\zeta = 1, 2, \dots$, where $\Omega(\zeta, J) = b_1^{(\zeta)}/(b_0^{(\zeta)} c_1)$ because $b_1^{(\zeta)}$ and $b_0^{(\zeta)}$ are also J -dependent with $J = k + 1/2$. This provides the level energies of the yrast band with $\zeta = 1$ corresponding to band A in Fig. 2, those in the next yrare band with $\zeta = 2$ corresponding to band B in Fig. 2, and so on. Since the spectrum is symmetric with respect to the $E = 0$ axis, only level energies with $E^{(\zeta)}(J) < 0$ with $\zeta = 1, 2, \dots$, need to be analyzed. Though $\Omega(\zeta, J)$ varies with J and ζ non-linearly, numerical analysis shows that it is almost a constant for a given ζ . As clearly shown in Fig. 2, $E^{(\zeta)}(J)/\chi$ for a given ζ uniformly follows a smooth curve described as a quadratic function of J . For example, the

level energies in the yrast band shown by curve A in Fig. 2 may be asymptotically given by

$$E^{(\zeta=1)}(J)/\chi = -J^2 + 0.413J - 0.0435 \quad (47)$$

for $J = 1/2, 3/2, \dots$; the level energies in the next yrare band shown by curve B in Fig. 2 may be asymptotically given by

$$E^{(\zeta=2)}(J)/\chi = -J^2 + 3.26J - 1.9 \quad (48)$$

for $J = 5/2, 7/2, \dots$, which are more accurate when J is large.

IV. SUMMARY

In this work, Bethe ansatz solutions of the two-axis countertwisting Hamiltonian for any (integer as well as half-integer) J are derived based on the Jordan-Schwinger (differential) boson realization of the $SU(2)$ algebra after the desired Euler rotations. It is shown that the solutions to the Bethe ansatz equations can be obtained more easily as zeros of the extended Heine-Stieltjes polynomials. It is verified that the zeros of the extended Heine-Stieltjes polynomials may be complex. Though we can not determine the imaginary parts of the zeros beforehand, the absolute values of the real parts of these complex zeros are all within the two open intervals $(0, 1)$ and $(1, c_1^{-2})$. Since each level is doubly degenerate for half-integer J due to time reversal symmetry, we only need to solve one of the cases. The results of the other case can be obtained by permuting the a -bosons with the b -bosons, which is efficiently helpful in determining all excited states of the system. However, unlike the procedure in [26] for integer J case, in which the $2J + 1$ solutions split into four sets of independent solutions, the procedure presented here gives rise to two sets of solutions with solution number being $J + 1$ and J respectively when J is an integer and being $J + 1/2$ each when J is a half-integer. It is clearly shown that double degenerate level energies for half-integer J case are symmetric with respect to the $E = 0$ axis. It is also shown that the excitation energies of the ‘yrast’ and other ‘yrare’ bands defined can all be asymptotically given by quadratic functions of J , especially when J is large. Our procedure may be used in calculating physical quantities of the system in order to produce maximal squeezed spin states of many-particle systems, especially when the number of particles is large.

Acknowledgments

Support from U.S. National Science Foundation (OCI-0904874, ACI -1516338), U.S. Department of Energy (DE-SC0005248), Southeastern Universities Research Association, the China-U.S. Theory Institute for Physics with Exotic Nuclei (DE-SC0009971), National Natural Science Foundation of China (11375080 and 11675071), Australian Research Council Discovery Project DP140101492, and LSU-LNNU Joint Research Program (9961) is acknowledged.

-
- [1] M. Kitagawa and M. Ueda, Phys. Rev. A 47, 5138 (1993).
 - [2] D. J. Wineland, J. J. Bollinger, W. M. Itano, F. L. Moore and D. J. Heinzen, Phys. Rev. A 46, R6797 (1992).
 - [3] D. J. Wineland, J. J. Bollinger, W. M. Itano and D. J. Heinzen, Phys. Rev. A 50, R67 (1994).
 - [4] A. Sørensen and K. Mømer, Phys. Rev. Lett. 86, 4431 (2001).
 - [5] J. Hald, J. L. Sørensen, C. Schori and E. S. Polzik, Phys. Rev. Lett. 83, 1319 (1999).
 - [6] I. D. Leroux, M. H. Schleier-Smith and V. Vuleć, Phys. Rev. Lett. 104, 073602 (2010).
 - [7] C. D. Hamley, C. S. Gerving, T. M. Hoang, E. M. Bookjans and M. S. Chapman, Nature Phys. 8, 305 (2012).
 - [8] H. Strobel, W. Muessel, D. Linnemann and T. Zibold, Science 345, 424 (2014).
 - [9] V. Meyer, M. A. Rowe, D. Kielpinski, C. A. Sackett, W. M. Itano, C. Monroe and D. J. Wineland, Phys. Rev. Lett. 86, 5870 (2001).
 - [10] J. Estève, C. Gross, A. Weller, S. Giovanazzi and M. K. Oberthaler, Nature 455, 1216 (2008).
 - [11] J. Appel, P. J. Windpassinger, D. Oblak, U. B. Hoff, N. Kjægaard and E. S. Polzik, PNAS 106, 10960 (2009).
 - [12] M. H. Schleier-Smith, I. D. Leroux and V. Vuleć, Phys. Rev. Lett. 104, 073604 (2010).
 - [13] H. Bethe, Z. Phys. 71, 205 (1931).
 - [14] L. Takhtajan, L. Faddeev, J. Sov. Math. 24, 241 (1984).
 - [15] V. Korepin, N. Bogoliubov, A. Izergin, Quantum Inverse Scattering Method and Correlation Functions, Cambridge monographs on Mathematical Physics (Cambridge University Press, 1993).

- [16] M. Gaudin, J. Phys. (Paris) 37, 1087 (1976).
- [17] R. W. Richardson, Phys. Lett. 3, 277 (1963); J. Math. Phys. 6, 1034 (1965).
- [18] R. W. Richardson and N. Sherman, Nucl. Phys. 52, 221 (1964).
- [19] P. Ribeiro, J. Vidal and R. Mosseri, Phys. Rev. Lett. 99, 050402 (2007).
- [20] P. Ribeiro, J. Vidal and R. Mosseri, Phys. Rev. E 78, 021106 (2008).
- [21] F. Pan and J. P. Draayer, Phys. Lett. B 451, 1 (1999).
- [22] H. Morita, H. Ohnishi, J. da Providência and S. Nishiyama, Nucl. Phys. B, 737, 337 (2006).
- [23] Y.-H Lee, J. Links and Y.-Z. Zhang, Nonlinearity 24, 1975 (2011).
- [24] M. A. Marchioli, D. Galetti and T. Debarba, Int. J. Quant. Inf. 11, 1330001 (2013).
- [25] F. Pan and J. P. Draayer, Ann. Phys. (N. Y.) 275, 224 (1999).
- [26] F. Pan, Y.-Z. Zhang and J. P. Draayer, Exact solution of the two-axis countertwisting Hamiltonian, arXiv: 1609.05581.
- [27] F. Pan, L. Bao, L. Zhai, X. Cui and J. P. Draayer, J. Phys. A 44, 395305 (2011).
- [28] X. Guan, K. D. Launey, M. Xie, L. Bao, F. Pan and J. P. Draayer, Phys. Rev. C 86, 024313 (2012).
- [29] F. Pan, B. Li, Y.-Z. Zhang and J. P. Draayer, Phys. Rev. C 88, 034305 (2013).
- [30] X. Guan, K. D. Launey, M. Xie, L. Bao, F. Pan and J. P. Draayer, Comp. Phys. Commun. 185, 2714 (2014).
- [31] A. Faribault, O. El Araby, C. Sträter, V. Gritsev, Phys. Rev. B 83 (2011) 235124.
- [32] O. El Araby, V. Gritsev, A. Faribault, Phys. Rev. B 85 (2012) 115130.
- [33] M. Bhattacharya, Analytical solvability of the two-axis countertwisting spin squeezing Hamiltonian, arXiv:1509.08530.
- [34] T. D. Thomas and J. R. Grover, Phys. Rev. 159, 980 (1967).